INL/CON-24-78260-Revision-0

Code Benchmark of Depressurized Conduction Cooldown Transient in the High Temperature Test Facility

November 2024

Robert Forrester Kile, Thanh Hua, Ling Zou, Sung Nam Lee, Geoff Waddington, Xianmin Huang, Tariq Jafri, Fajar Pangukir, Marek Stempniewicz, Ferry Roelofs, Zsombor Bali, Gusztv Mayer, Aaron S Epiney

Changing the World's Energy Future

INL is a U.S. Department of Energy National Laboratory operated by Battelle Energy Alliance, LLC

INL/CON-24-78260-Revision-0

Code Benchmark of Depressurized Conduction Cooldown Transient in the High Temperature Test Facility

Robert Forrester Kile, Thanh Hua, Ling Zou, Sung Nam Lee, Geoff Waddington, Xianmin Huang, Tariq Jafri, Fajar Pangukir, Marek Stempniewicz, Ferry Roelofs, Zsombor Bali, Gusztv Mayer, Aaron S Epiney

November 2024

Idaho National Laboratory
Idaho Falls, Idaho 83415

http://www.inl.gov

Prepared for the
U.S. Department of Energy
Under DOE Idaho Operations Office
Contract DE-AC07-05ID14517

Code Benchmark of a Depressurized Conduction Cooldown Transient in the High Temperature Test Facility

Robert F. Kile and Aaron S. Epiney
Idaho National Laboratory, Idaho Falls, ID, USA
1955 N. Fremont Ave, Idaho Falls, ID, 83415
robert.kile@inl.gov

Thanh Hua and Ling Zou
Argonne National Laboratory, Lemont, IL, USA
hua@anl.gov

Sung Nam Lee
Korea Atomic Energy Research Institute, Daejeon, Republic of Korea
snlee@kaeri.re.kr

Geoff Waddington, Xianmin Huang, and Tariq Jafri,
Canadian Nuclear Laboratories, Chalk River, Ontario, CA
geoff.waddington@cnl.ca

Fajar Pangukir, Marek Stempniewicz, and Ferry Roelofs
Nuclear Research and Consultancy Group, Arnhem, The Netherlands
pangukir@nrg.eu

Gusztáv Mayer
HUN-REN Centre for Energy Research, Budapest, Hungary
mayer.gusztav@ek.hun-ren.hu

Zsombor Bali
HUN-REN Centre for Energy Research, and
Budapest University of Technology and Economics, Budapest, Hungary
bali.zsombor@ek.hun-ren.hu

[leave space for DOI, which will be inserted by ANS]

ABSTRACT
We present results from modeling of a depressurized conduction cooldown (DCC) at the High Temperature Test Facility (HTTF) in the OECD-NEA Thermal Hydraulics Code Validation Benchmark for High-Temperature Gas-Cooled Reactors using HTTF Data. We briefly describe the benchmark and the models being used. We then present a comparison of steady state and transient results based on the Problem 2 Exercise 1A and 1B. We compare distributions of block and helium temperatures and coolant flow. We also compare energy balance in steady state. All models show comparable mass flow distributions and energy balances. The temperatures within the core and outer regions are comparable in all models too, but inner reflector temperatures can vary significantly. Despite that, we find that the models are in good agreement for the full-power steady state. In the DCC, we look at block temperature at the core midplane and RCCS water exit temperature. The INL and ANL models are found to be in excellent agreement with one another on block temperature over time, and when the KAERI and NRG models are considered agreement is good. Differences in the transient heat removal from the RCCS cause the differences in block temperature over time. The CNL models show similar trends to the INL, ANL, KAERI, and NRG models, but the temperatures are high because the volumes used in calculating the average temperature include the heater rods in the CNL models. The HUN-REN model shows slightly different RCCS behavior than other models, leading to differences in results, but these differences do not suggest fundamental differences.

KEYWORDS
Benchmark, HTTF, HTGR, system code, code-to-code comparison

1. INTRODUCTION

The High Temperature Test Facility (HTTF) is an integral effects high-temperature gas-cooled reactor (HTGR) thermal hydraulics test facility at Oregon State University (OSU) that is being used as the basis for a gas-cooled reactor thermal hydraulics benchmark. This benchmark, described in reference [1], contains exercises for code-to-code comparison between participants and for code validation based on experimental data. The benchmark contains three problems, one each capturing gas mixing in the lower plenum, the depressurized conduction cooldown (DCC), and pressurized conduction cooldown. Each problem also consists of at least two exercises. Exercise 1 is a code-to-code comparison exercise meant to assess the impact of modeling assumptions on code results among several participants. Exercise 2 is a code validation exercise where participants compare their results to HTTF data, and Exercise 3, which is only present for Problems 2 and 3, is for error scaling. This benchmark is being carried out by an international team of experts in systems codes, CFD modelling, and HTGRs. Participants in the work presented in this paper come from 5 countries.

Table I. HTGR T/H Benchmark Problems and Exercises. "Coupled" means systems codes models coupled to CFD models for the LP.

Problem Number	Physics	HTTF Experiment	Code-to-Code Exercise 1	Code-to-Data Exercise 2	Error Scaling, Exercise 3	Tools
1	LP Mixing	PG-28	Yes	Yes	No	CFD
2	DCC	PG-29	Yes	Yes	Yes	Systems, coupled
3	PCC	PG-27	Yes	Yes	Yes	Systems, coupled

This paper describes models built and results collected as part of Problem 2 Exercise 1 of the benchmark. This exercise is a code-to-code comparison exercise. Through code-to-code comparison, we can discuss results from each participant and gain insight into how different modelling techniques and closure relationships impact the results of each analysis. In this work, we found good agreement on block temperatures within the core region of HTTF in steady state but significant variations in temperature predictions in the inner reflector. We saw generally comparable behavior between most models during the DCC portion of the exercise, but there was some variation in results that merits further investigation.

2. MODELS USED

This paper presents seven sets of results using six different systems codes. Here, we provide a brief overview of each model. Prior to describing the models, we provide a brief overview of HTTF itself. Figure 1 shows a view of the core and part of the system. The core is made up of 10 blocks (numbered from the bottom up) of Greencast 94-F ceramic. The core is heated by 210 graphite resistive heater rods capable of generating up to 2.2 MW total power. The core contains 516 coolant channels through which helium can flow. Outside the core vessel is the reactor cavity cooling system (RCCS), which is composed of stainless-steel plates with water flow channels between them. The RCCS is separated from the reactor vessel by a cavity through which air can flow. Heat radiates from the reactor pressure vessel to the RCCS, which serves as the ultimate heat sink for long-term loss of flow transients. A detailed description of the facility can be found in reference [2].

2.1. Idaho National Laboratory (INL) RELAP5-3D Model

INL has modeled HTTF using a RELAP5-3D model developed from 2015-2018 [3]. A detailed description of the model can be found in reference [4]. This model divides the core itself into 3 radial zones (rings) containing coolant channels, heater rods, and core block. RELAP5-3D cannot model the HTTF block geometry exactly, so every region containing coolant channels is modeled using a unit-cell approach in which the volume of each component is preserved. Figure 2 shows the INL RELAP5-3D nodalization and the unit cells used. This model will be referred to as the INL model.

2.2. Argonne National Laboratory (ANL) SAM Model

ANL is modeling HTTF using their systems code SAM [5]. The ANL SAM model uses a two-dimensional (2D) ring approach to approximate the 3D geometry of HTTF. Rather than the unit cell approach used by INL, the SAM model consists of concentric rings of block, helium and heater rod material to approximately match the HTTF geometry. When the hexagonal shape of the core is converted to concentric rings, the surface area changes. This is accounted for in the model by applying a correction factor to the heat transfer surface area in the model.

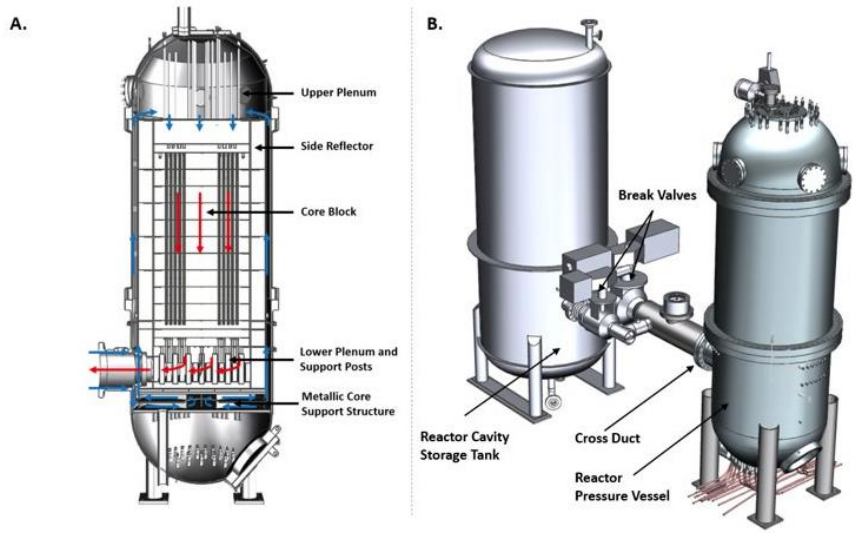

Figure 1. (A) A rendering of the core including flow paths (B) A system CAD model.

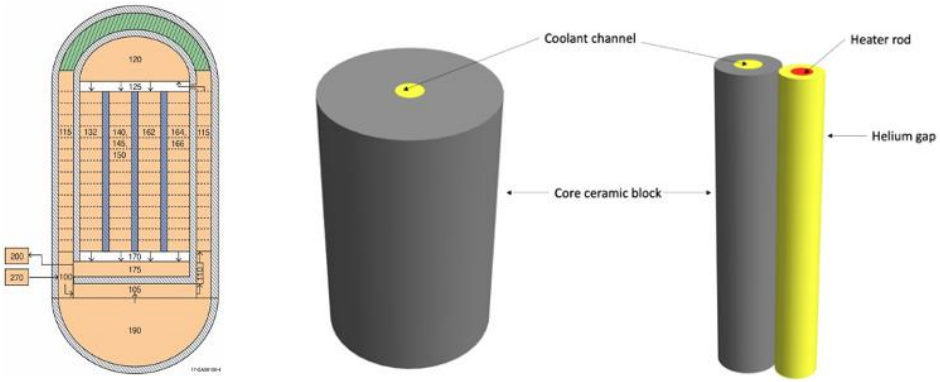

Figure 2. Nodalization diagram of the INL HTTF model (left) and unit cells for the reflector (center) and core (right).

Figure 3 shows the 2D ring model, which is described in greater detail in reference [6]. This model is referred to as the ANL model.

2.3. Korea Atomic Energy Research Institute (KAERI) GAMMA+ Model

GAMMA+ has been developing upgrades for the system transient and safety analysis of non-LWR reactors. GAMMA+ 2.0 has been released and is available for the analysis and design of HTGRs, Sodium-cooled fast reactors, Molten Salt Reactors, and Heat Pipe Reactors [7]. Figure 4 represents the GAMMA+ nodalization for HTTF system. The central and side reflector have 14 nodes axially and 3 nodes radially. The fuel blocks which contain the heater rod consist of 10 blocks (10 nodes axially). The fuel block divided into inner, middle and outer ring radially. This model is referred to as the KAERI model.

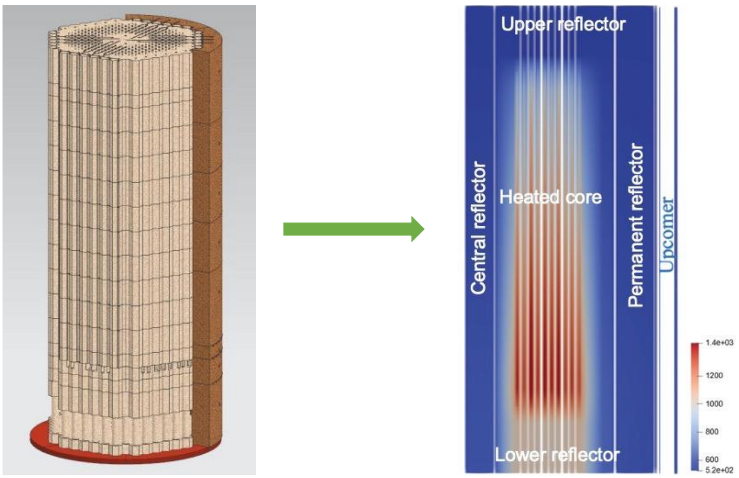

Figure 3. The SAM 2D ring model of HTTF.

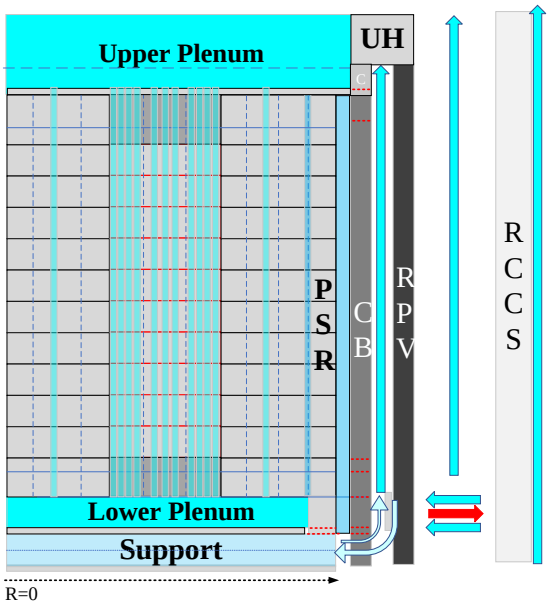

Figure 4. GAMMA+ nodalization (Blue: Fluid, Gray: Solid).

2.4. The Canadian Nuclear Laboratories (CNL) Models

CNL simulated the DCC benchmark with both RELAP5-3D and the CNL system TH code ARIANT. The HTTF models are similar for both codes, based on the concentric "cylindrical ring modeling" approach. There are separate rings representing the core ceramic region with embedded graphite fuel rods, and lumped coolant channels of four different sizes. The core is divided radially into 7 coolant channel groups (CGs) and eight solid core blocks (CBs), which include both the ceramic and graphite rods.

Figure 5 shows the ARIANT and RELAP5-3D models used for the P2.Ex1A and Ex1B benchmark cases. Both idealizations include open circuit models of the helium coolant loop and the water-cooled RCCS loop. The RELAP5-3D models include the air cavity loop, but this does not play a significant role. The five

parallel channel group models CG-1 to CG-5 represent the helium coolant channels through the core; the other parallel CG models represent the inner and outer bypass flows, and annular up-riser. The RELAP5-3D model includes a 3D component for the LP.

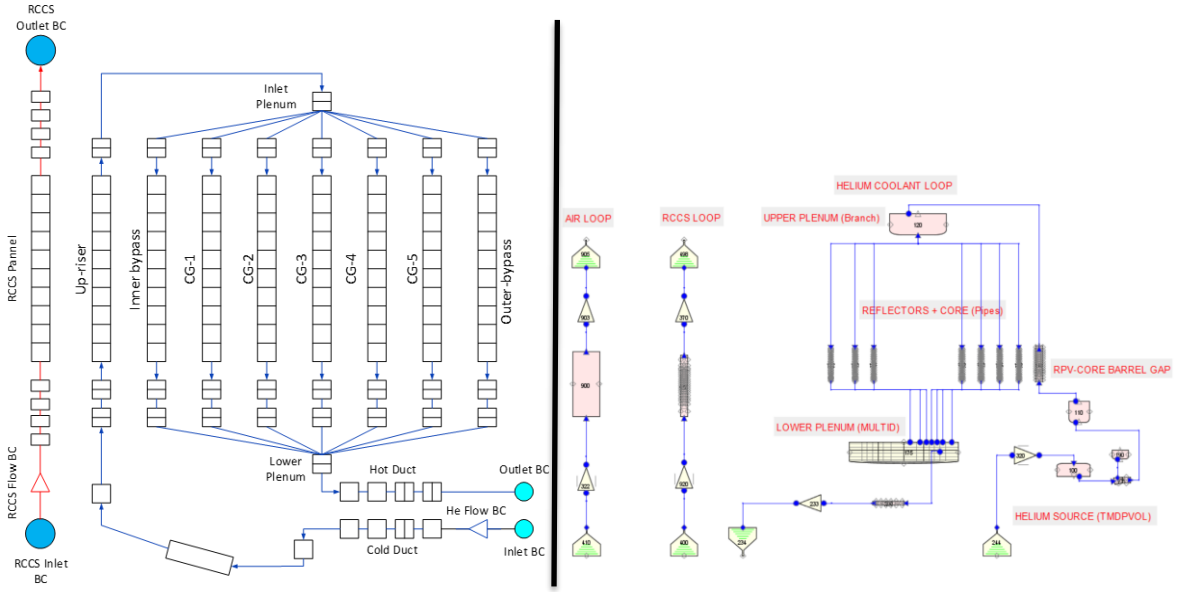

Figure 5. ARIANT (left) and RELAP5-3D (right) nodalization diagrams of HTTF. The black line separates the two models.

To model heat conduction in the solid elements, there are eight cylindrical core block models (CB0 through CB7). Models CB0 and CB7 represent, respectively, the inner and outer reflectors. Models CB1 through CB6 represent the core blocks between the inner and outer reflector, and each includes separate regions for the graphite heater rods and ceramic matrix. Convective heat transfer correlations are applied as boundary conditions between the solid CB models and the adjacent helium CG models. The CNL ARIANT model is referred to as the CNL-A model, and the CNL RELAP5-3D model is referred to as the CNL-R model.

2.5. The Nuclear Research and Consultancy Group (NRG) SPECTRA Model

SPECTRA (Sophisticated Plant Evaluation Code for Thermal-hydraulic Response Assessment) is a fully integrated system analysis code developed at NRG that models the thermal-hydraulic behavior of nuclear power plants [8]. This work used SPECTRA Version 24-02. In SPECTRA, HTTF is presented as concentric cylindrical rings consisting of graphite heater rods, ceramic blocks, helium coolant channels, side reflectors, a core barrel, a pressure vessel, a cold leg, a hot leg, and RCCS. The core is modelled using seven rings, and the eighth ring represents the vessel. The conversion of the annular ring from the original core block is based on conserving the cross-sectional area encompassed by the hexagonal pattern. In each heated ring, the number and size of helium coolant channels vary (small, medium, and large). In this respect, an equivalent diameter of the coolant channel is calculated to simplify the model, assuming each coolant channel uniformly receives 1/6th of the heat originating from the rod. The seventh ring is embedded in the outer reflector, the permanent side reflector, a 6 mm helium gap between the side reflector and the core barrel, and the core barrel itself. Figure 6 shows the radial nodalization and unit cell approach in SPECTRA. The main helium flow path entering the core comes from the gap between the barrel and the pressure vessel. Therefore, the 6 mm helium gap is modelled as a solid structure using helium thermal

conductivity and specific heat capacity. The last ring is the pressure vessel structure. This model is referred to as the NRG model.

2.6. The HUN-REN Centre for Energy Research CATHARE Model

Code Advance Thermohydraulique pour les Accidents des Reacteurs à Eau (CATHARE) is a French thermal-hydraulic system code developed by CEA, EDF, FRAMATOME, and IRSN [9]. It was originally written for simulating water-cooled reactors, but its validity was extended to gas-cooled reactors. CATHARE 3 was used in the present work.

In CATHARE, the HTTF is modelled with axial elements, volume elements, and wall-type thermal structures belonging to them. The cold duct, the upcomer, the hot duct, the RCCS, and the RCCS cavity are modelled with simple axial elements and walls, while the upper plenum, the lower plenum and the metallic core support structure are modelled by volume elements and walls.

The core itself is modelled with axial elements and walls, yet to capture radial and azimuthal effects, thermal connections had to be made between these elements. The methodology behind the discretization of the core was to split the whole core into six azimuthally identical regions, and then model the coolant and heater rod channels with identical sizes as one element. This way each azimuthal region (1/6 of the core) is represented by six axial elements: inner small coolant channel, inner medium coolant channel, heater rod channel, large coolant channel, outer medium coolant channel and outer small coolant channel. The axial elements' dimensions have been determined in a way as to reproduce the real flow sections and heated perimeters, while their walls have been scaled to represent the real volume of the corresponding regions of the core blocks. The inner and outer bypass regions are not separated azimuthally in the model, so one axial element and wall represent each region. This model is referred to as the HUN-REN model.

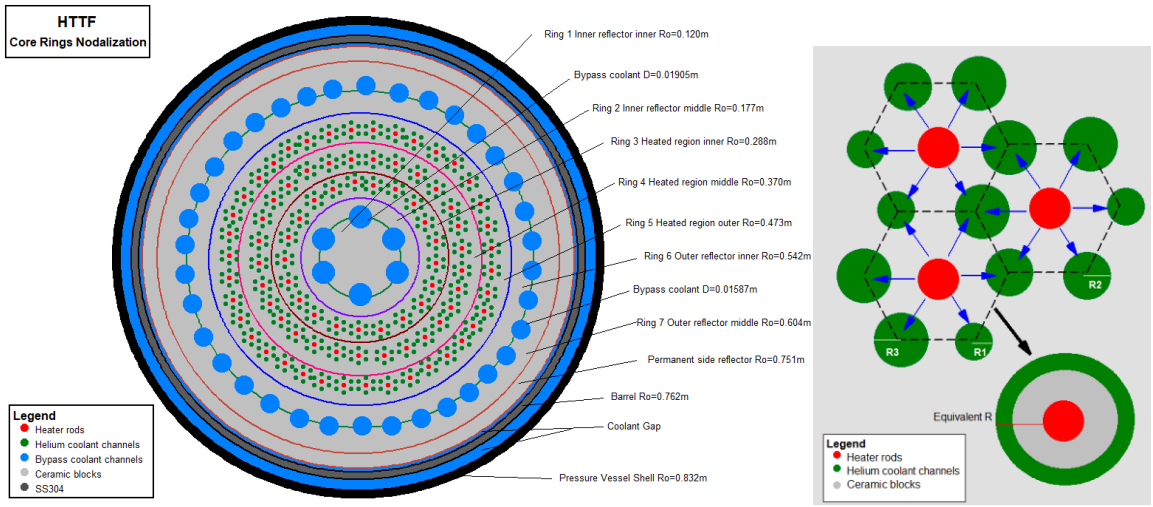

Figure 6. SPECTRA core nodalization (left) and unit cell approach (right).

3. RESULTS

Problem 2, Exercise 1 of the benchmark is divided into three sub-exercises. Exercise 1A represents a full-power steady state in HTTF, and Exercise 1B represents a DCC from full-power steady state. These conditions were never demonstrated in HTTF, but they provide a set of simple and consistent boundary

conditions for code-to-code comparison. Exercise 1C represents a DCC similar to the PG-29 experiment, but its input is more complex than that for exercises 1A and 1B. The benchmark specifications include thermophysical properties for the core materials to ensure consistency between benchmark participants. Here, we present the results for exercises 1A and 1B.

3.1. Exercise 1A: Full-power steady state

The full-power steady state boundary conditions are in Table II. Table III shows a comparison of energy balance results in the models. Good agreement in the energy balance is essential for comparing more detailed results such as temperature distributions. The largest difference in power removed by the primary helium is 6.9 kW, which amounts to 0.3% of the average value. The typical heat removal by the primary coolant is approximately 2186 kW. The CNL models did not include calculation of power removed by helium or the RCCS water. The KAERI model shows a total energy removal of 2204 kW, which is slightly greater than the steady-state power. This is likely a result of the approach for calculating heat removal. We are investigating these results further.

Table II. Full-power steady state boundary conditions

Parameter	Value
Power (MW)	2.2
Helium Flow Rate (kg/s)	1.0
Helium Inlet Temperature (K)	500.0
Helium Pressure (MPa)	0.7
RCCS Water Flow Rate (kg/s)	1.0
RCCS Water Inlet Temperature (K)	313.2
RCCS Water Pressure (MPa)	0.1
RCCS Cavity Air Flow Rate (kg/s)	0.025
RCCS Cavity Air Inlet Temperature (K)	300.0

Table III. Energy balance comparison between models in full-power steady state.

	Power Removed by Helium (kW)	Power Removed by Cavity Air (kW)	Power Removed by RCCS (kW)	Helium Outlet Temperature (K)	RCCS Outlet Temperature (K)
INL	2185.2	1.5	12.4	921.2	316.2
ANL	2186.9	2.3	14.9	920.5	316.7
KAERI	2188.7	1.3	14.2	921.5	316.6
CNL-A	-	-	-	-	-
CNL-R	-	-	-	916.6	315.8
NRG	2181.8	2.2	15.0	919.6	316.7
HUN-REN	2182.8	2.1	15.7	921.1	316.1

Figure 7 shows the block temperature profile as calculated by the various models. Radial positions under approximately 0.17 m are located in the inner reflector, and radial positions above 0.49 m but below 0.62 m are located in the outer reflector. Several differences between results stand out in Figure 7. The CNL RELAP5-3D model shows temperatures peaking as high as 1400 K. This is because the CNL RELAP5-

3D model includes both block and heater rod material in a single heat structure. The highest temperatures in the CNL RELAP5-3D model are the temperatures of the heater rods. The ANL model also shows a spiked pattern in block temperature. In this pattern the peaks are block temperatures close to the heater rods, and the valleys are block temperature farther away from the heater rods. There is a considerable spread in predicted inner reflector temperatures. This may indicate a need to review how radial conduction pathways are defined in systems code models. The NRG model has generally lower temperatures in all regions than the other models. One possible explanation for this difference requires a discussion of helium temperatures before it can be understood.

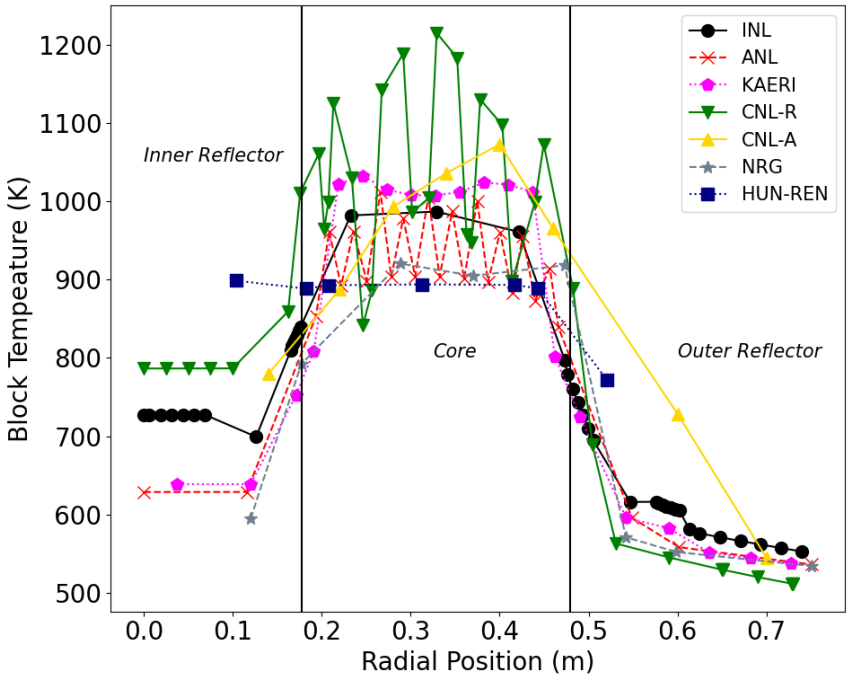

Figure 7. Block temperatures at the top of Block 5.

Figure 8 shows the helium temperature distribution in the models. The first matter of note is that the helium temperature in the core region in the NRG model is higher than in the other models. This, combined with the lower block temperature than the other models, strongly suggests that the NRG model is computing a heat transfer coefficient meaningfully higher than the other models. All models show low helium temperatures in the inner and outer reflector regions. The HUN-REN, ANL and KAERI models show relatively high helium temperatures at the inner and outer edge of the core region with a dip in helium temperature in the middle of the core region. The INL model shows a very slight dip in helium temperature in the middle of the core, but it is far less pronounced than in the HUN-REN, ANL and KAERI models. This behavior is the result of the coolant channel geometry in HTTF and the relatively fine radial nodalizations of the ANL and KAERI models. The innermost and outermost coolant channels in the core are smaller than the coolant channels in the middle of the core. This leads to greater friction in those channels and ultimately a higher power-to-flow ratio in those channels. In the middle of the core, the coolant channels are the largest, leading to a lower power-to-flow ratio and therefore lower temperatures.

Table IV shows the helium flow rates in the inner and outer reflectors and in the core. The core itself is divided into the inner, middle, and outer cores. The numbers and sizes of coolant channels in the inner, middle, and outer core are defined in the benchmark output templates. The bypass flow fraction is defined as the fraction of flow that goes through the reflectors instead of the core. Flow rates are mapped into the inner, middle, and outer rings according to the benchmark specifications. The CNL models show a significant temperature drop in the second of their five rings within the core. That ring has a total coolant flow of 0.217 kg/s, the highest flow in any of the five rings, despite having just 96 coolant channels. The rings further outward represent 114, 114, and 132 coolant channels, with varying diameters. A deep dive on mass fluxes may provide some illumination on this result, but it is not currently part of the benchmark. This significantly higher flow rate, despite a smaller number of coolant channels, explains the significant temperature drop in the CNL models in their second core ring. Overall, the mass flow rate distributions are very similar to one another in all the models, though the CNL models show a slightly higher flow in the inner core and slightly lower flow in the middle core when compared to other models.

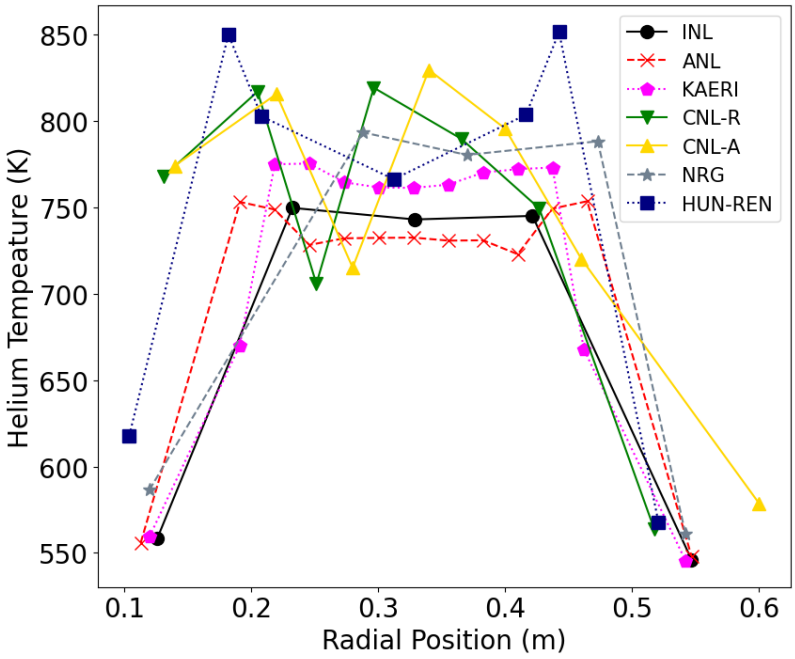

Figure 8. Helium temperatures at the top of Block 5

Table IV. Mass flow distribution comparison. Note that the bypass flow fraction may differ from what the reader can calculate from the table due to roundoff error.

	Inner Reflector (kg/s)	Inner Core (kg/s)	Middle Core (kg/s)	Outer Core (kg/s)	Outer Reflector (kg/s)	Bypass Flow (%)
INL	0.026	0.231	0.306	0.335	0.101	12.7
ANL	0.026	0.233	0.311	0.334	0.095	12.1
KAERI	0.025	0.224	0.309	0.344	0.097	12.2
CNL-A	0.018	0.255	0.264	0.356	0.104	12.2
CNL-R	0.021	0.255	0.274	0.350	0.101	12.2
NRG	0.022	0.229	0.317	0.333	0.099	12.1
HUN-REN	0.024	0.234	0.317	0.329	0.096	12.0

3.2. Depressurized conduction cooldown transient

The DCC occurs when the coolant pressure boundary is ruptured, and SCRAM occurs. This benchmark problem, the ANS-94 decay heat standard to simulate decay heat. The RCCS continues to operate at the conditions defined in Table II, and the core depressurizes from 0.7 to 0.1 MPa linearly over 20 seconds. During the DCC, heat transfer occurs through conduction and radiation. Axial conduction redistributes heat from the bottom of the core to the top, and radial conduction moves the heat through the block. Radiation heat transfer moves the heat from the block material through the barrel and vessel to the RCCS, which removes the heat from the system entirely. We compare the block temperature over time for the middle of the core during the DCC and the RCCS coolant outlet temperature. Figure 9 shows the block temperature at block 5 (core midplane) in the middle ring of the core region. The CNL models show significantly higher temperatures than the other models because the CNL temperatures are averaged over a volume that includes both block and heater rods. Notably, the CNL RELAP model shows a considerably slower cooldown than the other models do. The INL and ANL models agree with one another very well. The NRG and KAERI models both show an initial temperature rise within the first hour followed by a gradual cooldown over many hours but indicate different rates of heat removal than the INL and ANL models do. The block temperatures from the HUN-REN model show similar results to the KAERI model. The RCCS temperatures, which indicate heat removal from the core, shed some further insight and are shown in Figure 10.

The INL, ANL, KAERI, and NRG models show similar behavior, though over differing time scales. All 4 of those models show an initial decrease in temperature followed by a gradual increase until some peak, then temperatures drop again. In the NRG model, that peak occurs at approximately 16 hours. In the KAERI model, it occurs at approximately 25 hours. The INL and ANL models show that peak at approximately 19.5 and 23 hours respectively. The earlier peak temperature in the NRG model and the faster cooldown of blocks in that model indicate that heat removal to the RCCS is more effective in that model than in the other models. Similarly, the later peak in RCCS temperature in the KAERI model and the higher block temperature indicates a less effective RCCS. The HUN-REN RCCS temperature starts at a comparable value to the other models then drops lower than the other models before slowly rising again. Notably, the gradual cooldown following RCCS temperature peak is considerably slower in the HUN-REN model than in the other models.

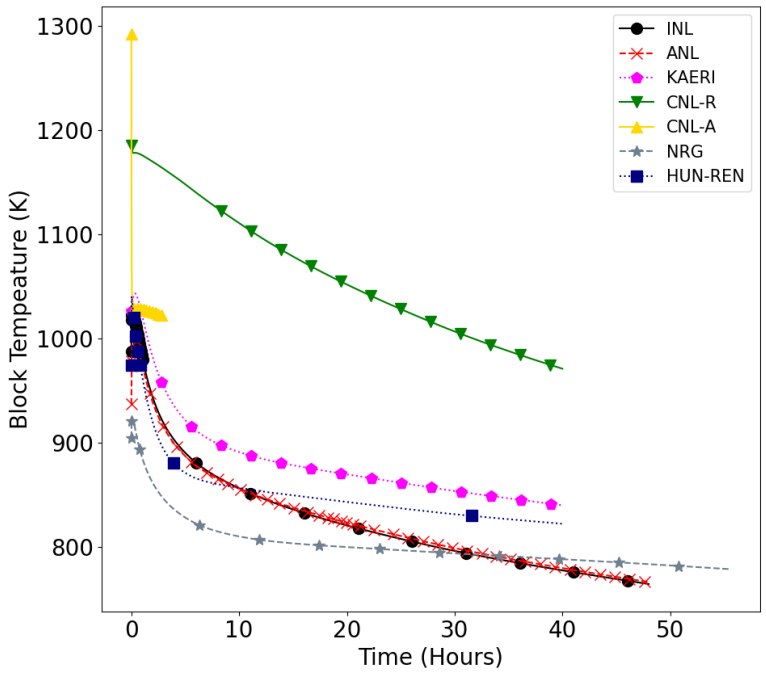

Figure 9. Block temperature over time in the middle ring at the core midplane.

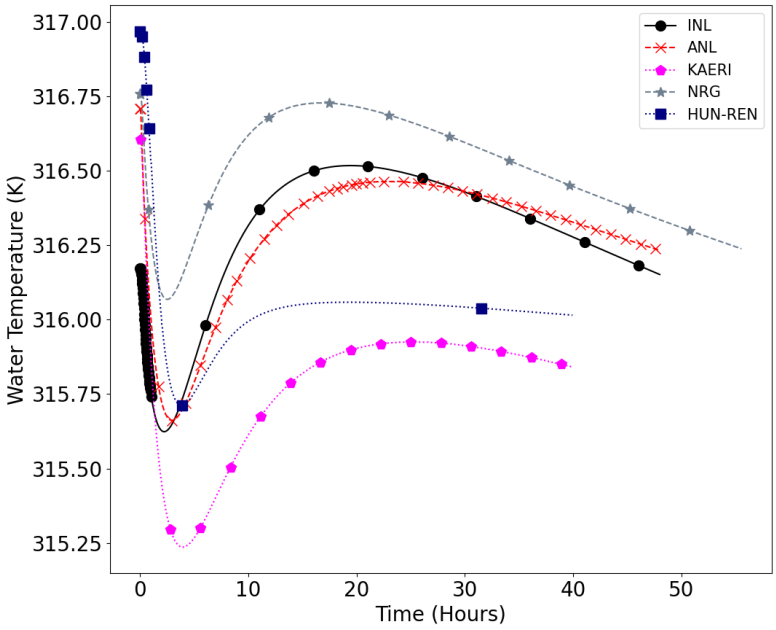

Figure 10. RCCS water exit temperature over time.

Overall, most models show comparable results for block temperature. The CNL models show higher temperatures, due to the inclusion of heater rod temperature in their average temperature. The INL and ANL models show incredibly similar results, while the KAERI and NRG models are similar to one another and the INL and ANL models, but varying heat removal to and by the RCCS leads to slightly different block cooldown rates. The RCCS temperatures and temperature evolution patterns are extremely similar for the INL, ANL, NRG, and KAERI models.

4. CONCLUSIONS

In this paper, we presented some results for Problem 2 Exercise 1A and 1B of the OECD/NEA HTGR T/H benchmark. Results from Exercise 1A indicated generally good agreement in energy balance and predictions of mass flow distribution. The CNL models indicated slightly higher flow in the inner ring of the core than other models, leading to lower temperatures in that region. Overall, temperatures in the core block material were similar. The difference between the hottest block material in the core and the coldest was 200 K, but those occurred at different locations. Temperatures in the inner reflector were considerably more varied, with a 342 K difference between the hottest and coldest temperatures. This suggests there may be a need for a systematic review of how conduction between the core and inner reflector is modeled.

The DCC results indicated extremely strong similarity between the INL and ANL models and strong similarity between the INL, ANL, NRG, and KAERI models. Temperatures in the CNL models are considerably higher in the core (CNL-R and CNL-A), but this is largely because the volume-averaged temperature shown includes heater rods and block material, whereas all other temperatures are only block material.

The HTGR T/H benchmark is still ongoing. Current results show good agreement among the models of many participants. Additional participants are developing solutions, and the participants in this paper may still revise their results before the publication of the final benchmark report. That report will be finalized December 2025 and will include a more thorough comparison of results from all participants using their final models for code-to-code and code-to-date exercises.

ACKNOWLEDGMENTS

The authors thank the OECD/NEA for providing the framework for this benchmark activity and the specifications for the benchmark problem carried out in this work.

INL: This work was funded by the U.S. Department of Energy Advanced Reactor Technologies Gas-Cooled Reactor (ART-GCR) program. This research made use of the Idaho National Laboratory's High Performance Computing systems located at the Collaborative Computing Center and supported by the Office of Nuclear Energy of the U.S. Department of Energy and the Nuclear Science User Facilities under Contract No. DE-AC07-05ID14517 This manuscript has been authored by Battelle Energy Alliance, LLC, under Contract No. DE-AC07-05ID14157 with the U.S. Department of Energy. The U.S. Government retains and the publisher, by accepting the article for publication, acknowledges that the U.S. Government retains a nonexclusive, paid-up, irrevocable, worldwide license to publish or reproduce this manuscript or allow others to do so for U.S. Government purposes.

ANL: This work is supported by the U.S. DOE Office of Nuclear Energy's Nuclear Energy Advanced Modeling and Simulation program. This manuscript was created by UChicago Argonne LLC, operator of ANL, which is a U.S. Department of Energy Office of Science laboratory operated under contract number DE-AC02-06CH11357.

KAERI: This work was supported by the National Research Foundation of Korea (NRF) grant funded by the Korea government (MSIT) (No. 2020M2D4A2067322).

CNL: The CNL effort was funded by Canadian Nuclear Laboratories (CNL) through its Laboratory Directed Science and Technology (LDST) Program, and by Atomic Energy of Canada Limited's (AECL) Federal Nuclear Science and Technology (FNST) Work Plan.

NRG: This project has received funding from the Dutch Ministry of Economic Affairs and Climate under NRG's R&D program, PIONEER.

REFERENCES

1. A. S. Epiney et al., "Overview of HTTF Modeling and Benchmark Efforts for Code Validation for Gas-Cooled Reactor Applications," *Proceedings of the 4th International Conference on Generation IV & Small Modular Reactors (G4SR-4)*, Toronto, Ont, Canada, October 3–6, (2022).
2. I. Gutowska, B. Woods, "OSU High Temperature Test Facility Design Technical Report, Revision 2," Oregon State University, Corvallis, OR, OSU-HTTF-TECH-003-R2 (2019). https://www.osti.gov/biblio/1599410.
3. The RELAP5-3D Code Development Team, "RELAP5-3D Code Manual Volumes I-V," Idaho National Laboratory, Idaho Falls, ID, INL/MIS-15-367323 (2018).
4. P. D. Bayless, "RELAp5-3D Input Model for the High Temperature Test Facility," INL/EXT-18-45579, Idaho National Laboratory, Idaho falls, ID, (2018). https://doi.org/10.2172/1811538.
5. R. Hu et al., "SAM Theory Manual," ANL/NSE-17/4/Rev. 1, Argonne National Laboratory, Lamont, IL (2022). https://doi.org/10.2172/1781819.
6. Z. Ooi, T. Hua, L. Zou, R. Hu, "Simulation of the High Temperature Test Facility (HTTF) Core Using the 2D Ring Model with SAM," *Nuclear Science and Engineering*, **197**(5), pp. 840–867, (2022). https://doi.org/10.1080/00295639.2022.2106726.
7. Lim, Hon Sik, "GAMMA+ 2.0 Volume I: User's Manual," Korea Atomic Energy Research Institute, Daejeon, South Korea, KAERI/TR-8663/2021 (2021).
8. M. M. Stempniewicz, "SPECTRA Sophisticated Plant Evaluation Code for Thermal Hydraulic Response Assessment, Version 24-02, Volume 1-4," NRG report K6223/24.277594 MSt-2402, Arnhem, The Netherlands (2024).
9. Préa Raphaël, et al., "CATHARE-3 V2. 1: The New Industrial Version of the CATHARE Code," *Advances in Thermal Hydraulics 2020*, pp. 730–742 (2020).